Electron Beam Effects on Polymers: V. Symmetric and Asymmetric Materials Based on the Controlled Distribution of bis-GMA into Crosslinked Nitrile Rubber Films Prior to Curing by Electron Beam Radiation

HA-CHUL KIM,[1] ABDEL M. EL-NAGGAR,[2] and GARTH L. WILKES*,[1]

[1]Department of Chemical Engineering and Polymer Materials and Interfaces Laboratory, Virginia Polytechnic Institute and State University, Blacksburg, Virginia 24061, and [2]National Center for Radiation Research and Technology, Cairo, Egypt

SYNOPSIS

Two systems based on the controlled distribution of the methacrylic acid derivative of the diglycidyl ether of bisphenol-A (bis-GMA) into crosslinked acrylonitrile–butadiene copolymers, commonly called nitrile rubber (NBR), were prepared utilizing electron beam (EB) radiation. In the system called "symmetric," the EB crosslinked NBR was swollen to equilibrium in solutions containing different concentrations of bis-GMA. The swollen NBR film was then EB irradiated to different dosage levels. The other system, called "asymmetric" or "gradient," was prepared by applying the solutions containing bis-GMA to *one surface* of the EB crosslinked NBR film in a controlled time that was less than the time to achieve an equilibrium concentration across the thickness or "swelling" dimension. This asymmetrically swollen NBR film was then immediately EB irradiated using different dose levels. The prepared symmetric and asymmetric NBR systems were investigated by thermal and mechanical, as well as microscopic, analyses. The mechanical responses were shown to be strongly dependent on the bis-GMA content in the NBR film and the type of preparation history. The dynamic mechanical spectra showed the presence of two transitions, indicating some level of phase separation that was supported by scanning electron microscopy of fracture surfaces for symmetric and asymmetric systems. The asymmetric distribution of the imbibed (cured) monomer in the asymmetric system was confirmed by both FT-IR and optical microscopy analyses.

INTRODUCTION

In the last decade, attention has been drawn to the area of polymeric material modification by blending to give a new material retaining some of the desirable features of each constituent polymer. Chemical modification based on various copolymerization methods leading to polymer blends or interpenetrating networks (IPN) have also been regarded as major directions in both the academic and industrial communications. Each modification method can be utilized to sometimes achieve a homogeneous in contrast to a multiphase system depending on the type of the desired ultimate applications. Numerous methods based on the chemical and physical modifications have been developed to generate multicomponent polymeric systems. Particularly, in recent years, the IPN concept offers unique potential features that provide a combination of various chemical networks and possibly a control of morphological structures.[1]

An IPN is defined as an alloy of two polymers produced by separate reactions and it can be prepared by two methods: sequential IPNs and simultaneous IPNs. For a sequential IPN, a prereacted network is swollen by another reactive monomer or functionalized oligomeric species and this system is then placed under conditions to polymerize the

* To whom correspondence should be addressed.

Journal of Applied Polymer Science, Vol. 42, 1107-1119 (1991)
 CCC 0021-8995/91/041107-13$04.00

added monomer. A simultaneous IPN, however, is generated from two networks formed by simultaneous polymerization.[2] Both types of IPNs have been utilized in producing toughened elastomers and reinforced plastics. The sequential IPN method can produce heterogeneous domains of various sizes depending on the system variables, such as the compatibility of the chemical components and the process conditions, etc.[3] In this latter case, which is of interest in our study, one polymeric material forms the matrix while the other constituent material may generate phase-separated particles and an interpenetrating network through crosslinking reactions. In a similar context, there has been a growing interest in the concept of generating systems of "asymmetric" or "gradient" structures utilizing the above-mentioned methodology based on IPN techniques and radiation processes.[4-6]

The gradient system, termed by Shen and Bever,[7] can be defined as a system in which structure and properties vary continuously and gradually. If this concept is applied to polymer film and coating technology, the final product might be asymmetric in that the structure and properties are changing gradually across the "film thickness dimension." Possible applications of the asymmetric gradient polymer films can be envisioned for a number of different fields, as qualitatively discussed by Shen and Bever.[7] The following examples are based on their discussion. Utilizing chemical properties, a reactive hydrophilic monomer could be diffused from one surface to the other through the hydrophobic polymer film generating a gradient concentration and subsequently polymerized. This method might conceivably result in a gradient of hydrophilicity across the hydrophobic polymer film thickness. A possible application was suggested, but not demonstrated, for the construction of gasoline tanks for aircraft or automobiles. A hydrophilic interior layer would help prevent the gasoline from swelling the material, while a hydrophobic exterior layer would be inert to water or moisture in the environment. As another example, now considering mechanical properties, if a relatively soft (rubbery) material is to be fastened to a rigid structure, the region where the fastener is to be applied requires higher mechanical strength. This can be achieved by obtaining a gradient of the glassy polymer across the rubbery polymer film. Other possible applications include utilizing surface modification to enhance resistance to abrasion and indentation, biocompatibility for medical applications, barrier properties such as for membrane technology, etc. After the introduction of the concept of the gradient polymeric system, Shen and coworkers published on the preparation and characterization of this system using crosslinked polystyrene and poly(methyl methacrylate) as substrates and acrylate monomers as penetrants.[4] In their studies, the polymer substrates were immersed in the monomer solutions for several days and exposed to ultraviolet radiation.

The objective of this study is to demonstrate the feasibility of preparing asymmetric materials. To achieve this, we have prepared and characterized two different systems, symmetric (serving as a control) and asymmetric, based on crosslinked nitrile rubber as an initial matrix. In the symmetric system, the NBR in the crosslinked (gel) form was swollen to equilibrium in a solution of the methacrylic acid derivative of the glycidyl ether of bisphenol-A (commonly called bis-GMA) followed by electron beam (EB) radiation. The obtained distribution of crosslinked bis-GMA inside the NBR matrix will be referred to as symmetric distribution even though, on a localized basis, some phase separation may occur. In the case of the asymmetric distribution, a solution of bis-GMA was allowed to partially penetrate the NBR films from *one surface only for a limited time that was less than the time to achieve a uniform concentration in this same direction.* The asymmetrically swollen NBR film was then immediately exposed to EB irradiation. This asymmetric system can be also called a gradient structure as previously mentioned. Schematic illustrations of the

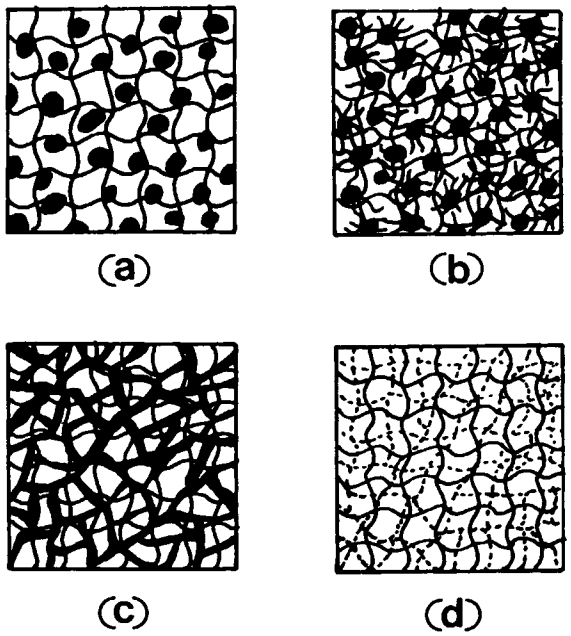

Figure 1 Schematic illustrations of possible morphological structures of NBR/bis-GMA symmetric systems.

morphological textures one might expect for some possible symmetric and asymmetric distribution of bis-GMA into the NBR matrix, or any other related two component systems prepared in a similar way, are shown in Figures 1 and 2. As illustrated, four possible sample morphological textures might result, discussed as follows. In the first case, as shown in Figure 1(a), the addition of the bis-GMA system, which is glassy in nature following crosslinking, might result in phase separation in the NBR matrix. The final properties would be dependent on the particle size, volume fraction, and size distribution of the dispersed glassy phase, as well as the chemical nature of the matrix and the dispersed phase.[8] One might expect that possibly the swollen unreacted system would be initially homogeneous; however, at a certain conversion, bis-GMA-rich domains could begin to form in the matrix if chemical immiscibility exists prior to possible vitrification of the bis-GMA component. In radiation curing, the phase-separation process becomes more complicated and significantly system dependent. This is due to the fact that the reaction generally proceeds rapidly with a temperature increase (due to exothermic reactions and radiation energy dissipation) until the system reaches vitrification resulting from diffusion limitation. A second case is illustrated in Figure 1(b), which exhibits a similar phase-separated morphology with the exception that the second polymerized particulate phase is interconnected by a network of its own kind. On the other hand, depending on the volume fraction of the dispersed glassy phase and the variables of the radiation curing process such as dose rate, a morphological structure similar to that shown in Figure 1(c) might result. In this case, the dispersed glassy phase is continuously connected by crosslinking but no distinct particulate regions occur. Finally, interpenetrating networks without significant phase separation might be a fourth possible texture, as schematically shown in Figure 1(d). The respective morphological structures of the symmetric system can be similarly modified as the asymmetric systems showing a concentration gradient across the thickness direction, as represented in Figure 2(a)-(d).

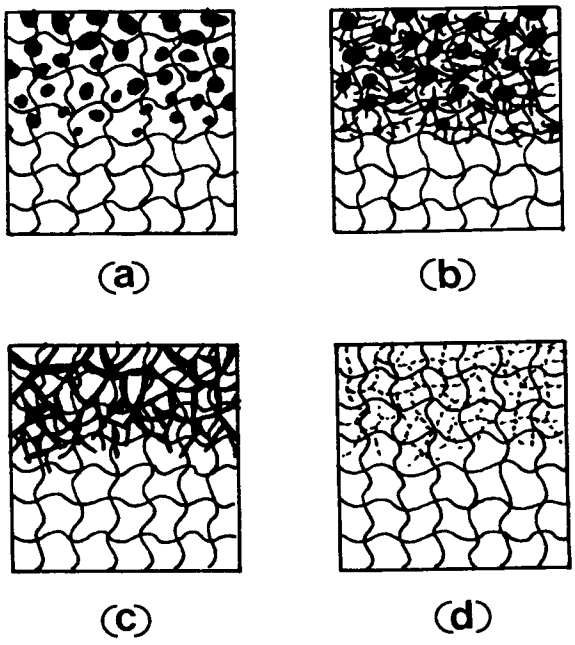

Figure 2 Schematic illustrations of possible morphological structures of NBR/bis-GMA asymmetric systems.

While the hypothetical morphologies represented in Figures 1 and 2 do not display signs of radiation grafting between the networks, this certainly is a possibility for also altering physical properties. The level of radiation grafting will, of course, be dependent upon the relative rates of radiation crosslinking between the two species making up the corresponding two networks. While this will be not treated in the oncoming paper, recognition of this difference in radiation grafting with different choices of starting materials should be noted.

MATERIALS AND EXPERIMENTS

Materials

Samples of an uncrosslinked acrylonitrile–butadiene copolymer (NBR, 40% acrylonitrile) were kindly provided by Dow Chemical Company. The number average molecular weight was 85,000 and its glass transition temperature was found to be ca. −20°C. This material was cured by EB irradiation and served as the crosslinked rubber matrix (the preparation of the crosslinked NBR is described later). Bis-GMA was obtained in the form of a viscous liquid from Freeman Chemicals (Nupol 46-4005). The chemical structures of these materials are shown in Figure 3. Tetrahydrofuran (THF) and acetone (HPLC grade) were purchased from Fisher Scientific.

Electron Beam Irradiation

Electron beam irradiation was carried out at room temperature under a nitrogen atmosphere. An electrocurtain accelerator manufactured by Energy Science, Inc. (model CB/150/115/180) was used

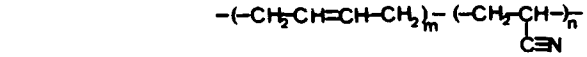

(a)

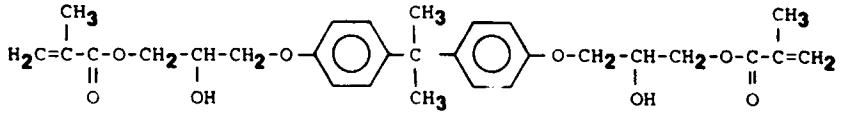

(b)

Figure 3 Chemical structures of (a) acrylonitrile–butadiene copolymer (NBR) and (b) bis-GMA.

throughout this study. The samples were placed on steel plates in aluminum trays and passed through the conveyor system of the electron beam instrument. The maximum available dose per pass was 20 Mrad; hence, for the highest dosage used in this study (40 Mrad), two passes were required.

Preparation of Crosslinked NBR Film Samples

Thin films (4–5 mil in thickness) of the initially uncrosslinked NBR were prepared by first dissolving the NBR linear polymer in THF and casting at room temperature. These NBR films were then EB irradiated following the procedure mentioned above. The gel formation was evaluated by immersing and stirring the irradiated NBR film in THF for 72 h and subsequently drying the network film at vacuum for 72 h. Figure 4 shows the influence of irradiation dose on the gel formation. It can be seen that, over the dose range studied, the gel percent reaches a value of approximately 90% at 30 Mrad. A further dose to 40 Mrad causes little increment in gel content. Hence, in this study, NBR film samples cured by an EB dose of 40 Mrad were utilized as the crosslinked rubber matrix without further extraction of the sol fraction (ca. less than 10%).

Swelling Procedures

The dry extracted NBR gels were then immersed in bis-GMA–acetone solution for controlled lengths of time. The swollen NBR samples were then removed from the solutions, gently wiped, and dried at vacuum to a constant weight to remove the acetone. The weight uptake of bis-GMA was determined as follows:

$$\% \text{ wt uptake} = \frac{\text{dried NBR wt after swelling} - \text{initial NBR wt}}{\text{initial NBR wt}} \times 100.$$

This procedure was applied to the symmetrically swollen NBR films. The swelling behavior of these NBR gels in the bis-GMA containing solution as a function of time is presented in Figure 5. It is seen that the bis-GMA weight uptake by NBR gel film increases significantly by increasing the bis-GMA concentration in acetone up to 50%.

It is apparent that the time for equilibrium swelling of the NBR gel depends on the bis-GMA concentration. The equilibrium swelling time was found to increase from 5 min for the 5% bis-GMA solution to 120 min for the 50% solution. Based on the results presented in Figure 5, NBR films carrying 17, 36, 79, and 117% weight uptake of bis-GMA (these values based on the initial dry NBR weight) were prepared to be irradiated for the symmetric systems.

An asymmetric distribution or gradient structure of the bis-GMA through the NBR film was prepared by allowing the swelling solution to contact *only* the upper surface. *The penetration (swelling) of the bis-GMA solution was controlled by leaving the bis-GMA solutions for a limited time that was less than the time to achieve equilibrium swelling.* This controlled time is also dependent on the concentration of the

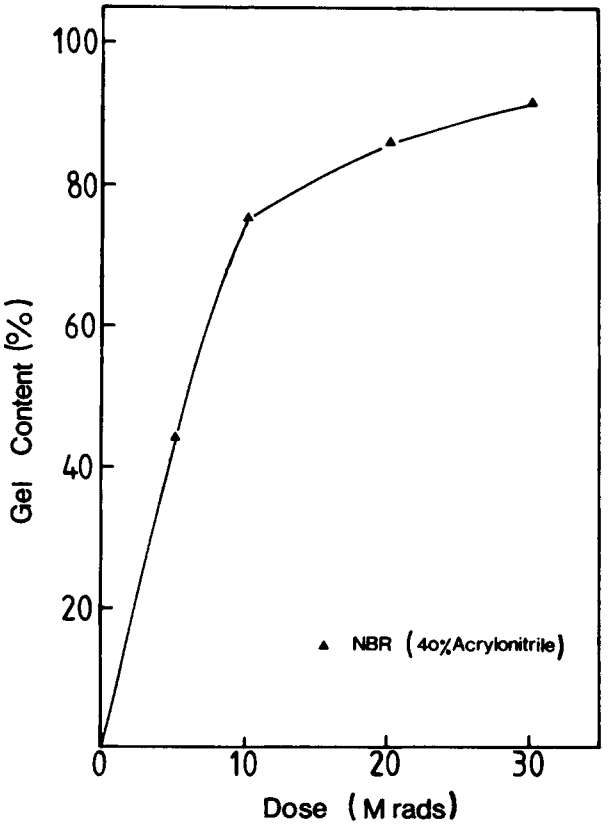

Figure 4 Effect of EB radiation dose on the gel formation of NBR.

swelling bis-GMA solution as shown previously in Figure 5. As an example, swelling times of 5 min for the 25% solution or 10 min for the 10% solution were utilized to obtain the asymmetric concentration gradient based on the results in Figure 5. The partially swollen NBR film was immediately exposed to EB irradiation after the excess solution on the upper film surface had been gently wiped away. No consideration was made for the possible influence of any remaining acetone on the radiation-induced reaction in the NBR film that had been swollen with bis-GMA and acetone. There may be some influence of the acetone in the respect that it might undergo some reaction, particularly by the carbonyl group in this moiety.

Mechanical Properties

The irradiated samples were tested to determine Young's modulus, elongation, and tensile strength at break at ambient temperature. Samples were cut with a die in a dogbone shape with the initial dimensions being 10 mm in gauge length and 2.8 mm in width. An Instron tensile tester (model 1122) was used with an extension rate of 50% per minute based on the initial sample length. Young's modulus was calculated from the initial slope of the stress–strain curves. The tensile strength was obtained at the break point. Dynamic storage and loss moduli (E' and E''), as well as tan δ, were determined as a function of temperature using an Autovibron Dynamic Viscoelastometer. These samples were run from −40–200°C to investigate the thermal transition behavior with a scanning rate of 2°C/min at a frequency of 11 Hz.

Thermal Properties

Differential scanning calorimetry (DSC) measurements were performed using a Perkin–Elmer DSC-4 Calorimeter equipped with a TADS data station. An indium standard was utilized to calibrate the temperature scale. A heating rate of 10°C/min was used and the determinations were performed under a nitrogen atmosphere. A given sample was run from 15 to 75°C; this initial scan was labeled "first run." After that sample was cooled to 15°C with a cooling rate of 10°C/min, the sample was reheated to 75°C at the same scan rate. This scan was labeled "second run."

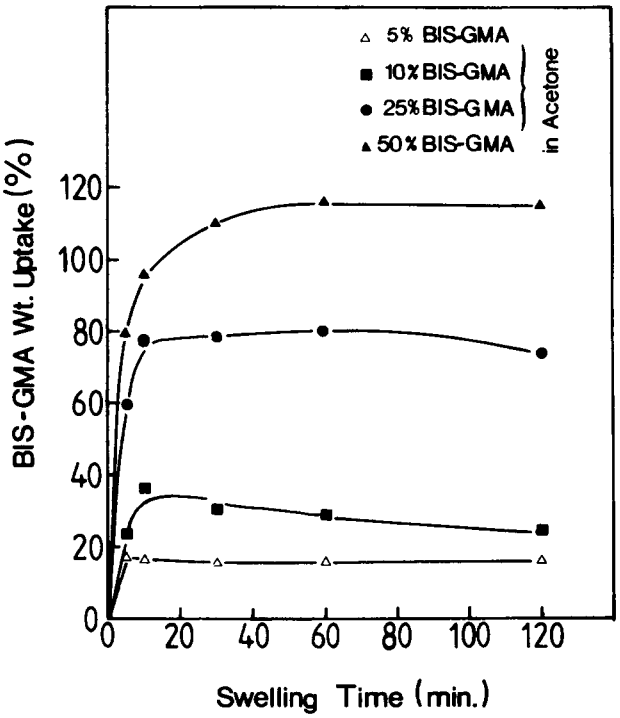

Figure 5 Swelling behavior of crosslinked NBR in solutions containing different concentrations of bis-GMA.

Scanning Electron Microscopy Analysis

The morphological structure of the EB-irradiated NBR systems was investigated using scanning electron microscopy (SEM) of fractured surfaces. The SEM micrographs were taken with a Cambridge Stereoscan 200 instrument. The EB irradiated NBR/bis-GMA samples were first fractured in liquid nitrogen and then sputter coated with gold. The SEM technique was utilized as one means to investigate the symmetric and asymmetric distributions of crosslinked bis-GMA that occurred inside the NBR matrix.

FTIR Microscopy Analysis

Symmetric and asymmetric distributions of bis-GMA inside the NBR film were investigated using an FT-IR spectrometer (Nicolet model 5DXB) equipped with a Spectra-Tec IR-PLAN infrared microscope. The movable apertures were set to 40 microns by 40 microns in size. First, an NBR film was precisely cut in a direction perpendicular to the film surface, resulting in a strip 125 microns (5 mils) in the original film thickness and a thickness (125 microns) in the direction perpendicular to the cross-section surface. Next, the original film thickness of the NBR film (ca. 125 microns) was divided into three regions (ca. a 40 μm $\times$ 40 μm square for each region)—these being called "lower," "middle," and "upper" regions in an order moving from the bottom to the top of the NBR film facing the cross-section. A schematic of the NBR film prepared for FT-IR microscopy is shown in Figure 6, which illustrates the details of the analysis. A FT-IR spectrum was obtained for each region and analyzed for the relative concentration distribution of bis-GMA throughout

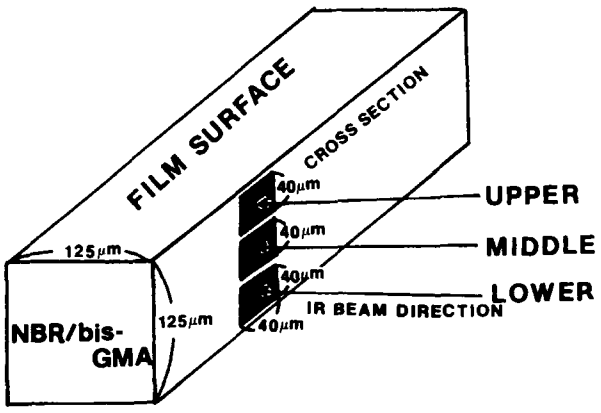

Figure 6 Schematic of the NBR sample prepared for the FT-IR microscopy analysis.

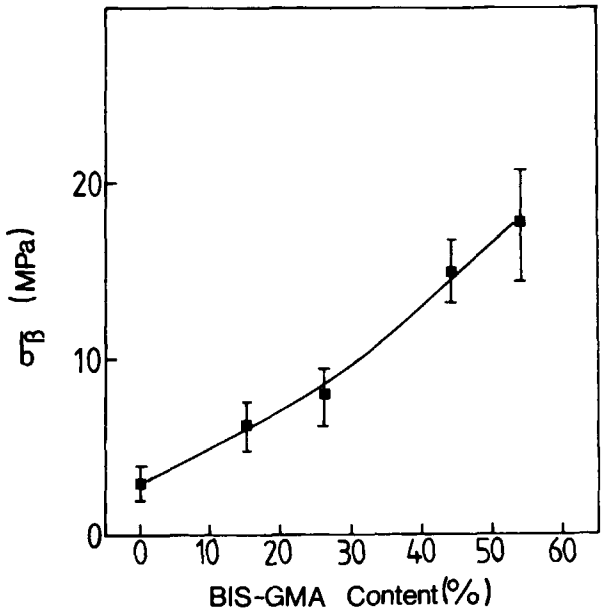

Figure 7 Tensile strength at break as a function of bis-GMA content in the NBR/bis-GMA symmetric system.

the thickness of NBR film. The phenyl peaks (1583 and 1608 cm^{-1}) from the presence of bis-GMA were normalized to the nitrile peak (2235 cm^{-1}) to account for variations in sample thickness.

Optical Microscopy Analysis

A Zeiss polarizing microscope equipped with a 35 mm camera was utilized to investigate the symmetric and asymmetric distributions of bis-GMA inside the NBR film. Thin strip samples of 5 mils in the original film thickness and 5 mils in the thickness perpendicular to the cross-section surface (as described in Fig. 6) were stretched to 30% elongation using the Instron. The stretched samples were then immediately released, relieving the mechanical strain on the NBR samples. The cross-section of the sample prepared as above was investigated with a microscope utilizing crossed polarizers for reasons discussed later.

RESULTS AND DISCUSSION

Symmetric Distribution of bis-GMA

Mechanical Properties

The mechanical properties of the EB-radiation-prepared symmetric NBR/bis-GMA films are shown in Figures 7, 8, and 9. Figure 7 presents the tensile strength of NBR/bis-GMA systems as a function

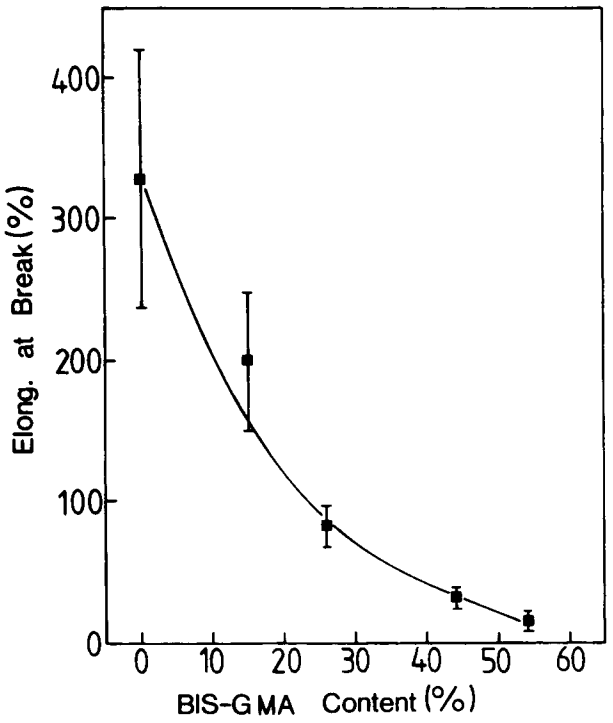

Figure 8 Elongation at break as a function of bis-GMA content in the NBR/bis-GMA symmetric system.

of bis-GMA content. In this plot, the zero point in the x-axis represents 100% NBR. It is clear that the tensile strength of the prepared material is significantly enhanced by increasing the bis-GMA content in the material. On the other hand, the elongation at break decreases dramatically, as might be expected by increasing the bis-GMA content as shown in Figure 8. Moreover, Young's modulus is markedly increased by increasing bis-GMA content in the prepared material, as illustrated in Figure 9. The increase in tensile strength and modulus upon increasing bis-GMA content can be explained on the basis of increasing the level of crosslinked bis-GMA material in the NBR matrix. This increased content reinforces the rubber phase and causes the decrease in elongation at break.

Dynamic Mechanical Properties

The EB curing process of an initially homogeneous mixture of epoxy resin (bis-GMA) and rubber (NBR matrix) can be generally represented by the sequential processes—phase separation, gelation, and vitrification—the exact order of which will depend upon several variables including composition, dose, etc. As the molecular weight of bis-GMA increases, the system undergoes *in situ* phase separation due to the lowered compatibility between the NBR and the poly(bis-GMA). Phase separation is generally terminated due to vitrification by which the crosslinking reaction becomes diffusion limited. These phenomena can be discussed in terms of the well-known time–temperature transformation (TTT) process[9] with the concept being applied in this laboratory to radiation curing.[10] These latter studies suggest that the free radicals trapped in the reacting network (bis-GMA) due to vitrification exhibit a finite lifetime. When a dynamic mechanical test is performed on a pure EB-cured (5 Mrad) bis-GMA with an aging time of a relatively short period (e.g., 1 h), two tan δ peaks may exist—a less pronounced one at about 55°C and the other at ca. 160°C.[10] This can be explained in terms of the TTT process as mentioned above. As the temperature scan proceeds in the dynamic mechanical tests, the cure temperature from the EB radiation process is surpassed. At this point, the material physically softens and simultaneously the bis-GMA component acquire chain mobility such that the activated species (e.g., trapped free radicals) can continue the crosslinking reaction—the combination of these two processes resulting in a *small* tan δ peak. Another tan δ peak exists at a higher temperature. That is, the continued chemical crosslinking after the initial softening point (ca. 55°C) during the relatively slow temperature scan (e.g., 2°C/min) provides the bis-GMA

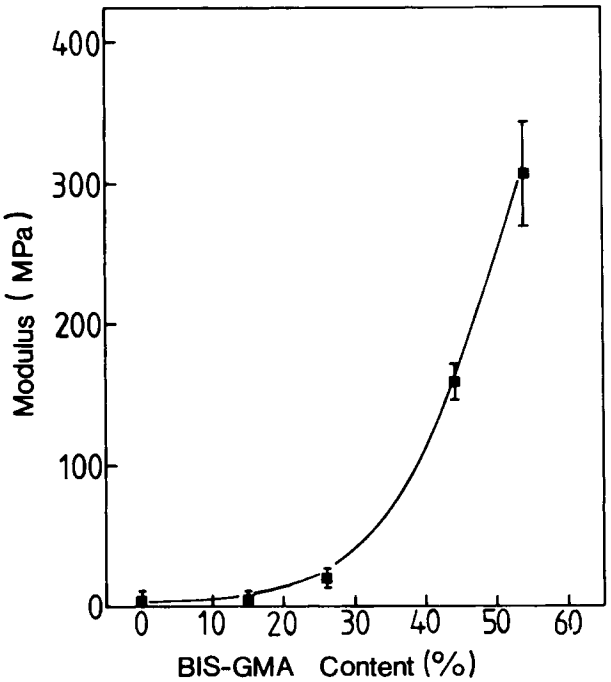

Figure 9 Young's modulus as a function of bis-GMA content in NBR/bis-GMA symmetric system.

with a near glassy modulus until the rate of reaction slows down at a higher temperature (ca. 160°C), where another tan δ peak occurs. This decrease in reaction rate is caused by the depletion of a sufficient concentration of reactive moieties (bis-GMA) in close proximity. However, in the case of longer aging times after EB irradiation (e.g., 120 h), the trapped free radicals recombine and/or are scavenged (likely by oxygen) such that the amount of further crosslinking during the temperature scan is reduced, resulting in the second tan δ peak at lower temperature in comparison to the case of the sample without aging. Details on these behavioral aspects were shown in a previous study from this laboratory.[10,11] The NBR/bis-GMA material for the dynamic mechanical analysis in this study were aged for at least several days, and therefore the material may soften (the second transition) at a slightly lower temperature (< 160°C for the 5 Mrad irradiated sample). This second T_g (maximum in tan δ peak) hereafter is referred to as the T_g of the EB cured bis-GMA component in the NBR/bis-GMA system.

Dynamic mechanical tests were performed on the

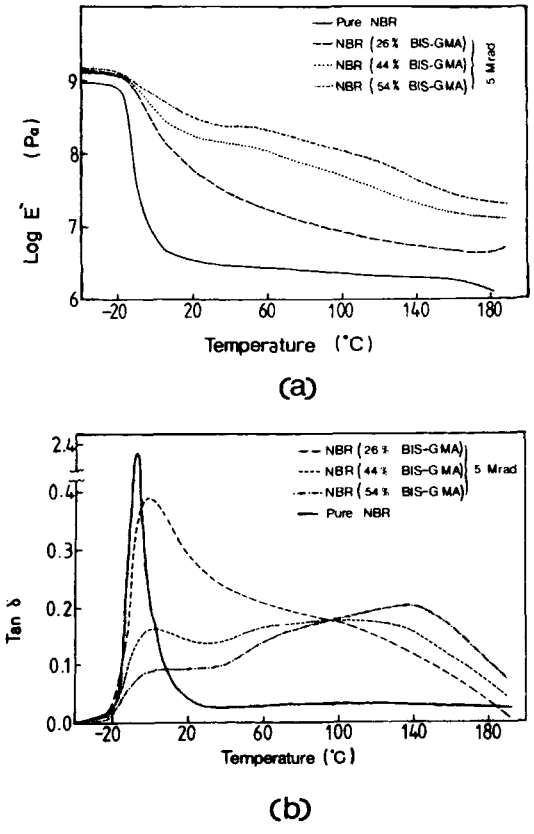

Figure 10 Dynamic mechanical spectrum of the symmetric NBR/bis-GMA (5 Mrad) system: (a) storage modulus (E') and (b) tan δ.

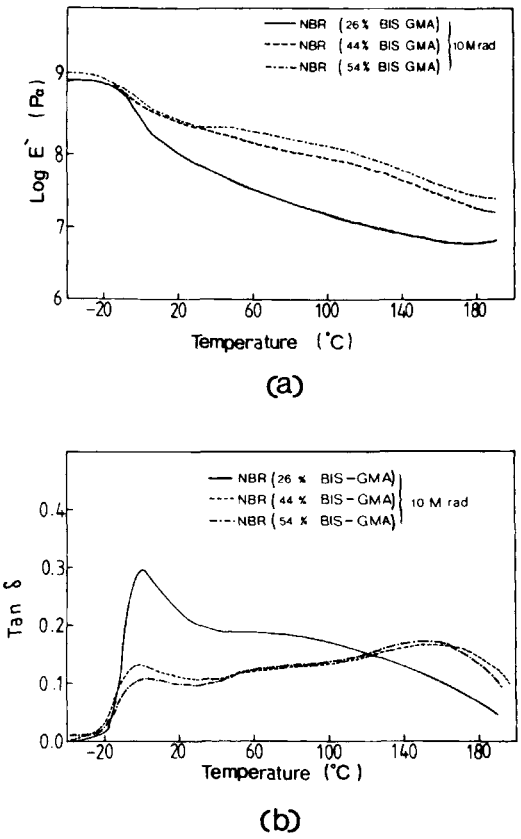

Figure 11 Dynamic mechanical spectrum of the symmetric NBR/bis-GMA (10 Mrad) system: (a) storage modulus (E') and (b) tan δ.

EB-prepared NBR systems to illustrate the existence of a symmetric distribution and possible phase separation of bis-GMA in the NBR matrix. Figures 10 and 11 show the temperature dependence of the storage modulus and tan δ for the systems containing different contents of bis-GMA prepared at 5 and 10 Mrads, respectively. From these dynamic mechanical spectra, two principal transitions can be identified. The lowest is due to the NBR glass transition that occurs around 0°C (maximum in tan δ). This transition is in agreement with the T_g obtained for crosslinked pure NBR as shown in Figure 10. A second transition occurs between 120 and 150°C (the location of this transition depends on the exact preparation condition as discussed earlier) that is attributed to the glass transition temperature of the irradiated pure bis-GMA.

The observation of two distinct transitions clearly suggests the occurrence of considerable phase separation of bis-GMA from the NBR phase during the EB curing process. It is obvious from the storage modulus plots (Fig. 10) that pure NBR initially shows a lower modulus in comparison to the bis-

GMA/NBR systems and, above the lower T_g (NBR), all samples display a rubbery plateau value. The modulus value for the rubbery plateau tends to increase with increasing bis-GMA content, as can be expected. It was shown that the NBR system containing 26% bis-GMA does not show distinct T_g characteristics for the bis-GMA component but rather displays a peak-broadening as shown in Figures 10 and 11. This significant broadening of the transition at the higher temperature in the NBR system may arise from some degree of grafting reaction between NBR and the bis-GMA and mixing of the two component networks. If grafting occurs, it likely occurs simultaneously with the crosslinking of bis-GMA component within the NBR matrix. The T_g (tan δ peak) of NBR is found to increase from −8°C at 5 Mrad to 2°C at 10 Mrad for the NBR sample of 26% bis-GMA. Also, the glass transition of the bis-GMA component in the systems having bis-GMA contents of 44 and 54% was found to increase with increasing radiation dose, indicating that the amount of cure of the bis-GMA is proportional to radiation dosage—again, an expected outcome. A summary of these results is presented in Table I, showing the effects of radiation dose and bis-GMA content on the dynamic mechanical properties.

Thermal Analysis

Figure 12 represents the DSC thermograms for pure NBR (40 Mrad) and NBR systems with different bis-GMA contents. All samples were aged at room temperature for 1 h prior to the DSC test. In general, the exothermic behavior is only observed for samples having higher bis-GMA contents than 15%. Table I also shows the heat of the exotherm, ΔH, as calculated from the exothermic peak area for NBR/bis-GMA systems prepared at 5 and 10 Mrad. It is obvious that the total area increases by increasing the bis-GMA content and decreases by increasing the dosage from 5 to 10 Mrad as shown in Table I. This exotherm can be easily explained as a result of

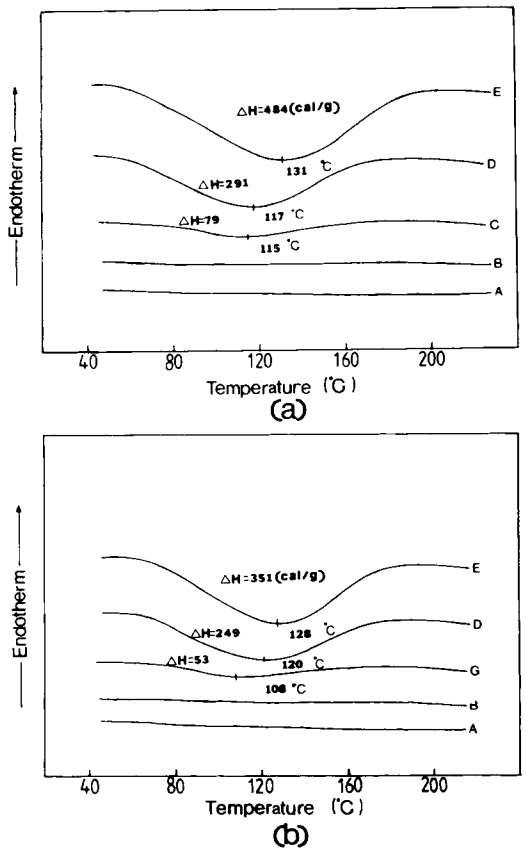

Figure 12 DSC scans of NBR/bis-GMA symmetric systems prepared at (a) 5 Mrad and (b) 10 Mrad: (A) pure crosslinked NBR and NBR/bis-GMA containing (B) 15%, (C) 26%, (D) 44%, and (E) 54% bis-GMA.

the further crosslinking of bis-GMA that occurs from trapped free radicals formed during EB irradiation and crosslinking from thermally induced opening of double bonds during the DSC experiments. One notes that the initial scan shows no sign of a glass transition temperature. Based on earlier studies from our laboratory on partially cured bis-GMA through radiation curing, it is the onset of the exotherm that provides a good index of the upper

Table I Dynamic Mechanical and Thermal Properties of NBR/bis-GMA Symmetric Systems

bis-GMA Content (%)	EB Radiation Dose (Mrad)	NBR Glass Transition (°C)	bis-GMA Glass Transition (°C)	Exothermic Heat ΔH (cal/g)
26	5	−8	—	79
	10	2	—	53
44	5	0	117	290
	10	−2	156	249
54	5	0	136	484
	10	2	156	351

temperature region associated with the glass transition distribution.[11] These findings were confirmed by a second DSC scan, which showed no exothermic peak but only a "flat" response. Moreover, these results are in accordance with a previous study from this laboratory that showed that the exotherm at higher temperature occurs from the thermally induced reaction of residual double bonds in bis-GMA.[11]

SEM Analysis

A SEM micrograph of the fractured surface of the NBR/bis-GMA material having 20% bis-GMA content is shown in Figure 13. Small particles dispersed throughout the fractured surface of the NBR matrix indicate that some amount of the bis-GMA has phase-separated, although the volume percent of the particles by themselves clearly do not appear to represent the amount of 20% bis-GMA content. As can be expected, some portion of bis-GMA that may not have participated in the phase separation would remain dispersed within the NBR network, as might be suggested by the morphological texture given earlier in Figure 1(b).

Asymmetric Distribution of bis-GMA

Mechanical Properties

Mechanical properties of the asymmetric or gradient NBR/bis-GMA systems having different bis-GMA content (10, 20, and 35%) are shown in Table II. These materials were prepared by subjecting one surface of the NBR film to a bis-GMA solution for 5 min, quickly removing any excess solution from the surface, and following immediately by EB irradiation at a 10 Mrad dose. As expected, the tensile strength at break as well as the Young's modulus again increased with increasing bis-GMA content, while the elongation at break decreases.

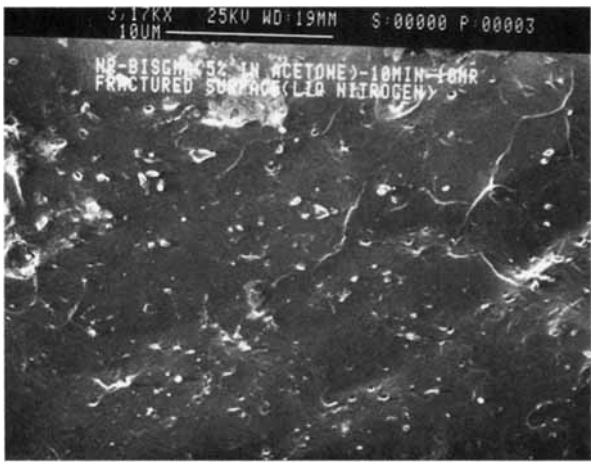

Figure 13 SEM photograph of fractured cross-section of the NBR/bis-GMA symmetric system.

Table II Mechanical Properties of NBR/bis-GMA Asymmetric Systems

bis-GMA Content (%)	Tensile Strength (MPa)	Young's Modulus (MPa)	Elongation at Break (%)
10	3.4	6.7	117
20	3.6	12.5	61
35	4.9	13.1	73

Dynamic Mechanical Properties

Figures 14 (a) and (b) show the temperature dependence of the storage modulus and damping (tan

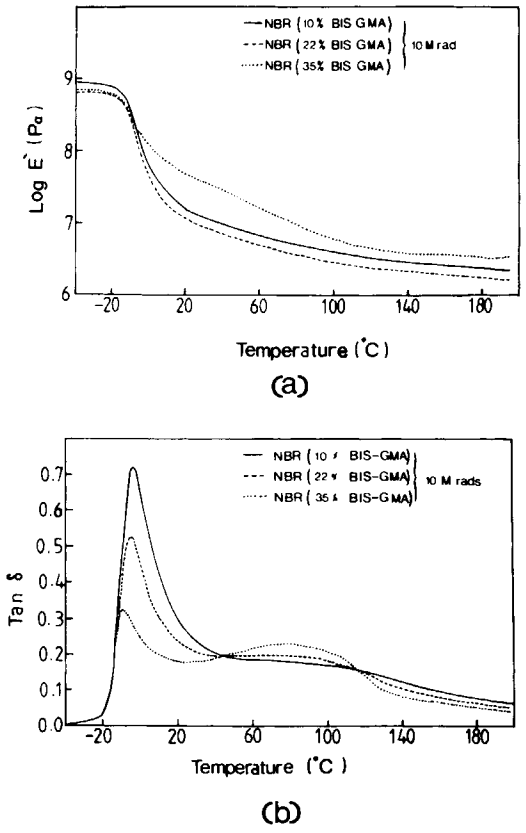

Figure 14 Dynamic mechanical spectrum of the asymmetric NBR/bis-GMA system: (a) storage modulus (E') and (b) tan δ.

Figure 15 SEM photograph of fractured cross-section of the NBR/bis-GMA asymmetric system. Top of photograph is the surface by which bis-GMA penetrated.

δ) for three asymmetric NBR/bis-GMA samples having different contents of bis-GMA. The transition at lower temperatures (−10–0°C) is distinct and arises from the NBR phase as previously discussed. On the other hand, the second transition due to the presence of bis-GMA in the NBR material occurs from 50–120°C. In comparison to the dynamic mechanical spectra of the symmetric system (Figure 11), the tan δ peaks of the higher or second transition are significantly broadened and somewhat shifted to lower temperature. To explain this, the anticipated morphological structure of the NBR/bis-GMA should be described. In any of these films, one expects to have a concentration distribution of bis-GMA across the NBR matrix. At the upper surface where the bis-GMA solution was initially introduced, both NBR and bis-GMA phases should be present and then gradually the concentration of bis-GMA should decrease in the direction as the bottom surface is approached. Therefore, the significant broadening of the second transition shown in Figure 14 is tentatively attributed to the gradient structure in sample morphology. However, further support for this speculation will be provided later.

SEM Analysis

Figure 15 shows a SEM of the fractured surface of a NBR/bis-GMA sample possessing a asymmetric distribution. Small particles dispersed near the upper surface of the NBR matrix indicate that a considerable amount of the bis-GMA has phase-separated. It also shows a "concentration gradient" distribution of the phase-separated bis-GMA particles across the NBR film "thickness" supporting the earlier discussion. Therefore, this SEM micrograph strongly indicates that an asymmetric distribution of bis-GMA phase has resulted with a certain degree of phase separation as proposed previously.

FT-IR Microscopy Analysis

Table III shows the results obtained from the FT-IR microscopy investigation, which clearly illustrate the distribution of the bis-GMA in the NBR/bis-GMA material. Two peaks at the respective wavelengths of 1583 and 1608 cm^{-1} due to the presence of the phenyl ring in bis-GMA were normalized to the peak at 2235 cm^{-1} ($-C \equiv N$) from the NBR material. These ratios are shown for the three regions, upper, middle, and lower (as schematically shown in Figure 5 and explained earlier).

For the asymmetric systems, the concentration of bis-GMA decreases gradually from the upper (near surface) region to the lower region (near bottom) as demonstrated by a decreasing phenyl ring content. This decreasing tendency was shown from both peaks at 1583 and 1608 cm^{-1}. These data from FT-IR microscopy analysis affirm the earlier more indirect dynamic mechanical as well as SEM results supporting our discussion that gradient or asymmetric distribution in the NBR film was present.

Table III FTIR Microscopy Data for the NBR/bis-GMA Systems

Sample	Analysis Region	Peak 1 (2235/cm)	Peak 2 (1583/cm) (Peak 2/Peak 1)	Peak 3 (1608/cm) (Peak 3/Peak 1)
Asymmetric	Upper	1.73	0.29 (0.17)	0.83 (0.48)
	Middle	2.25	0.23 (0.10)	0.61 (0.27)
	Lower	2.42	0.17 (0.07)	0.42 (0.17)

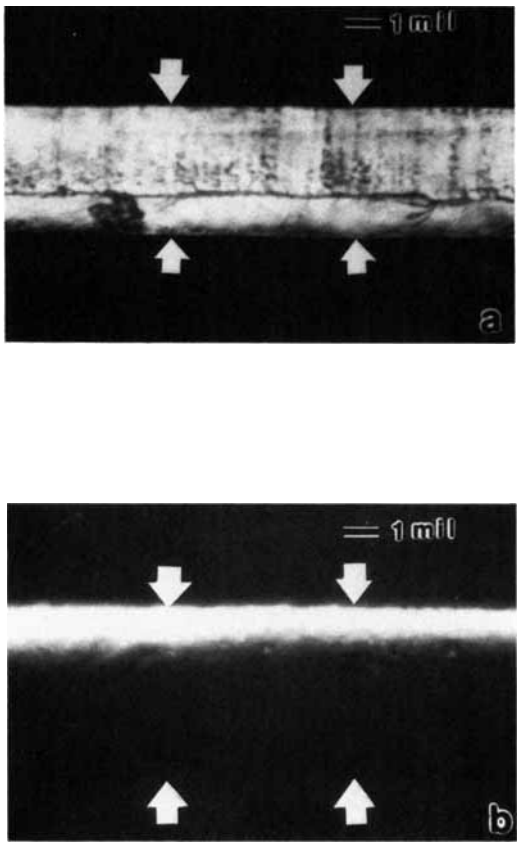

Figure 16 Cross-polarized optical micrographs showing the cross-sections of (a) symmetric and (b) asymmetric NBR/bis-GMA samples. In the asymmetric material, the bis-GMA penetrated the upper surface.

Optical Microscopy Analysis

Cross-polarized optical micrographs were taken to observe the cross-sections of the symmetric and asymmetric NBR/bis-GMA films. As discussed earlier, the samples were stretched to 30% elongation followed by immediate release of the strain prior to the microscopy studies. The purpose of this stretching and releasing procedure was to generate mechanically induced residual anisotropy (chain orientation) in the NBR/bis-GMA systems. Pure NBR material displays optical anisotropy (birefringence) when it is stretched; however, this anisotropy disappears immediately after the mechanical strain is released reflecting the loss of orientation. In contrast, the NBR/bis-GMA system retains the optical anisotropy after the mechanical strain is released due to the glassy nature of the EB cured bis-GMA distributed inside the NBR film that prevents the NBR matrix from recovering its initial dimension in a relatively short time period. This preparation procedure generating the mechanically induced residual anisotropy was expected to help demonstrate the symmetric and asymmetric distribution pattern of bis-GMA in the NBR matrices.

Figures 16(a) and (b) show the cross-polarized optical micrographs of the cross-sections of the symmetric and asymmetric NBR films, respectively. The symmetric sample [Fig. 16(a)] shows a brightness (birefringence) evenly distributed across the NBR film, indicating that bis-GMA is symmetrically distributed. In striking contrast, the asymmetric sample shown in Figure 16(b) resulted in a gradient of the induced birefringence across the NBR film. The bright surface region and the decreasing brightness toward the bottom surface obviously demonstrate that a gradient concentration distribution of bis-GMA was obtained for the asymmetric system. Although these observations on the distribution of the mechanically induced anisotropy are qualitative, they clearly represent the distribution pattern of bis-GMA inside the NBR matrix. Hence, the results of this investigation are in strong agreement with the thermal, mechanical, SEM, and FTIR microscopy analysis.

CONCLUSION

Symmetric and asymmetric systems based on the controlled distribution of the bis-GMA into a network acrylonitrile–butadiene copolymer (NBR) were prepared utilizing electron beam (EB) radiation. In the symmetric system, the crosslinked NBR was swollen to equilibrium in a bis-GMA–acetone solution followed by EB irradiation. In the case of asymmetric system, only one surface of the EB crosslinked NBR film was exposed to a bis-GMA–acetone solution for a limited time that was less than the time to achieve a uniform concentration profile in the swelling direction. The asymmetrically swollen NBR film was then immediately cured by EB irradiation. The mechanical tests showed that the final properties were strongly dependent on the bis-GMA content of NBR/bis-GMA systems. The dynamic mechanical studies showed the presence of two major transitions, suggesting a considerable degree of phase separation of bis-GMA inside the NBR matrix for both symmetric and asymmetric systems. The prepared symmetric and asymmetric distributions of bis-GMA in the NBR/bis-GMA systems were demonstrated by dynamic mechanical tests but particularly by FT-IR, SEM, and optical microscopy analyses.

Financial support for this study from the 3M Corp. is gratefully acknowledged.

REFERENCES

1. K. C. Frisch, H. L. Frisch, D. Klempner, and S. K. Mukherjee, *J. Appl. Polym. Sci.*, **18,** 689 (1974).
2. L. H. Sperling, in *Interpenetrating Polymer Network and Related Materials,* Plenum, New York, 1981.
3. J. K. Yeo, L. H. Sperling, and D. A. Thomas, *Polymer,* **24,** 307 (1983).
4. G. Akovali, K. Biliyar, and M. Shen, *J. Appl. Polym. Sci.*, **20,** 2419 (1976).
5. S. Yamakawa and F. Yamamoto, *J. Appl. Polym. Sci.*, **22,** 2459 (1978).
6. F. Yamamoto and S. Yamakawa, *J. Polym. Sci., Polym. Phys. Ed.*, **17,** 1581 (1979).
7. M. Shen and M. B. Bever, *J. Mater. Sci.*, **7,** 741 (1972).
8. C. K. Riew, *Rubber Chem. Technol.*, **54,** 374 (1981).
9. L. C. Chan, J. K. Nae, and J. K. Gillham, *J. Appl. Polym. Sci.*, **29,** 3307 (1984).
10. D. Thompson, Ph.D. thesis, Virginia Polytechnic Institute and State University, 1986.
11. D. Thompson, J. H. Song, and G. L. Wilkes, *J. Appl. Polym. Sci.*, **34,** 1063 (1987).

Received March 2, 1990
Accepted April 23, 1990